Available online at www.sciencedirect.com
SCIENCE DIRECT
Polymer 46 (2005) 5385–5395
polymer
www.elsevier.com/locate/polymer

Fibrillation of thermotropic liquid crystalline polymer enhanced by nano-clay in nylon-6 matrix

Baoqing Zhang[a], Yanfen Ding[a], Peng Chen[a], Chenyang Liu[a], Jun Zhang[a], Jiasong He[a,*], Guo-Hua Hu[b,c]

[a]*Key Laboratory of Engineering Plastics, Joint Laboratory of Polymer Science and Materials, Institute of Chemistry, Chinese Academy of Sciences, Beijing 100080, People's Republic of China*
[b]*Laboratory of Chemical Engineering Sciences, CNRS-ENSIC-INPL, 1 rue Grandville, BP 451, 54001 Nancy, France*
[c]*Institut Universitaire de France, Maison des Universités, 103 Boulevard Saint-Michel, 75005 Paris, France*

Received 1 February 2005; received in revised form 14 March 2005; accepted 17 March 2005
Available online 25 April 2005

Abstract

The influence of well-dispersed nano-clay filler on the morphology of thermotropic liquid crystalline polymer (TLCP) in nylon-6 matrix was investigated by melt extrusion process. The good dispersion of clay in the hybrid blends was confirmed by X-ray diffraction, transmission electron microscopy and rheological measurement. Morphological observation showed that the clay platelets had dramatic influences on the dispersion and deformation of TLCP phase. The TLCP droplets got smaller at the clay content ≤ 3 wt%, and deformed into fibrils at the clay content up to 5 and 7 wt%. The morphology evolution of TLCP in the hybrid blends, especially at 7 wt% of clay loading, was consistent well with the prediction based on the micro-rheology parameters such as the viscosity ratio of the dispersed phase to the matrix (η_d/η_m) and the ratio of capillary number to the critical capillary number (Ca/Ca_{crit}). This enhanced fibrillation of TLCP droplets was attributed to the role of nano-clay particles as a compatibilizer to improve the interfacial adhesion and to suppress the interfacial slip between TLCP and nylon phases in the melt, so that the shear stress was effectively transferred to the dispersed TLCP phase.

Keywords: TLCP blends; Morphology; Nylon-6 nanocomposites

1. Introduction

Since the emergence of aromatic liquid crystalline co-polyesters [1], polymer blends containing thermotropic liquid crystalline polymers (TLCPs) have received significant attention from the academic and industrial fields. Extensive studies on this topic have been carried out, and some review articles concerning various aspects of this kind of blends are available in the literature [2–5].

It is worth noticing that, even at the beginning of the studies on this kind of blends, researchers had tried to introduce inorganic reinforcements into such blend systems [6,7]. The addition of inorganic fibers could not only enhance the mechanical properties of the blends but also reduce the anisotropy of resulted materials [8]. Rheological testing revealed that TLCPs could reduce the melt viscosity of glass-filled thermoplastics [7,9,10]. When the TLCP component was deformed into fibrils in situ during the melt processing of ternary composites containing a solid reinforcement, the composites were named as in situ hybrid composites [11,12]. Much work has been published regarding the studies on TLCP-containing systems with different inorganic solid reinforcements, such as glass fibers [13,14], carbon black [15,16], whisker [17,18] and silica [19,20]. Most of above researches paid attention mainly to the balance between mechanical properties and processability of such filled TLCP blends, though other properties were also in consideration (e.g. the conductivity of the system, in Ref. [16]).

In order to obtain high strength, high modulus and heat-resistant materials, a high loading (up to 30–50 wt%) of conventional solid reinforcement is needed in such a hybrid composite. Therefore, the lightweight merit of in situ

* Corresponding author. Tel.: +86 10 6261 3251; fax: +86 10 8261 2857.
E-mail address: hejs@iccas.ac.cn (J. He).

0032-3861/$ - see front matter © 2005 Elsevier Ltd. All rights reserved.
doi:10.1016/j.polymer.2005.03.093

composites is lost because of the relatively high density of conventional solid reinforcement (ca. 2.5 g/cm^3) compared to that of TLCPs' (ca. 1.4 g/cm^3). On the other hand, the dispersion of silicate platelet at nanometer scale thickness in a polymer matrix can lead to higher reinforcing efficiency and good thermal-resistant properties even at very low loading levels (typically <10 wt%), as a result of their high specific surface area and aspect ratio [21,22]. But in order to obtain the composite with super mechanical properties, the matrix with high viscosity is frequently needed to promote the exfoliation of silicate platelets [23]. A masterbatch preparing process has been developed to balance the exfoliation degree and the melt viscosity. However, the lowing of viscosity was realized by trading-off the modulus of the composites [24]. Based on the roles that the TLCP plays in the reinforced polymer blends [12,13,17], blending the nanocomposite of high viscosity with a TLCP is the feasible method to improve its processability while do not harm its mechanical properties. Therefore, the combination of TLCP and silicate platelet reinforcement is a promising way to develop in situ hybrid composites that inherit almost all the advantages of the in situ composites and the filler-reinforced composites, with good processability, low density and high mechanical properties at the same time.

Moreover, the interactions between the dispersed TLCP droplets and silicate platelets with one of its dimensions in nanometer scale in a polymer blend have not been reported yet, although the role of organoclay as a compatibilizer in immiscible polymer blends has been the focus of some researches in recent years [25–31]. A distinct appearance for the compatibilization effect is the dramatic decrease of the dispersed domain size with the addition of organoclay. Though the physical mechanism behind the compatibilizing effect of the clay in immiscible polymer blends is still not very clear, it is commonly accepted that the effect originates from both thermodynamic and kinetic factors [28]. The thermodynamic factor may be induced by the interaction of clay with both polymer components at the interphase as that a block polymer compatibilizer does. In addition, the thermodynamic effect may appear as the thermal property change of the components, such as the shift of T_gs towards each other [25]. In a given polymer blend, it is possible that only the kinetic factor contributes to the compatibilization effect. As the situation in the nylon-6/EPR system, Khatua suggested that the steric hindrance effect from the exfoliated clay plates prevented the coalescence of the dispersed phase [30]. A concise review on the topic of clay filled immiscible polymer blends can be found in a recent publication of Ray et al. [31].

If the minor component in a polymer blend changes from a flexible-chain polymer to a rigid one as the TLCP, what effects will be brought by the organoclay to the dispersed phase? Does the compatibilizing effect of the organoclay also exist in a TLCP-containing blend? If the compatibilizing effect exists in such a blend, what could be manifested besides the decrease of dispersed domain size?

To answer these questions, clay filled polymer blends with a TLCP as the minor phase were prepared in this study. Nylon-6 was chosen as the thermoplastic matrix because of the easy exfoliation of organic silicate layers in it by using melt-blending method [32–34]. Furthermore, some interesting interactions of fillers (i.e. glass fiber, glass bead) with the dispersed TLCP in Nylon-6 matrix and consequential influences on the morphology and rheological properties of hybrid systems were reported from our laboratory [35,36]. Nylon-6 nanocomposites with well-dispersed silicate platelets were prepared by melt extrusion using a twin-screw extruder. Then nylon-6 nanocopmosites with different clay loadings were melting blended with a commercial TLCP (Vectra A950 from Hoechst Celanese) at temperatures above its melting point. The morphological observation showed that the introduction of silicate platelets had significant effects on the morphology of the TLCP phase. The fibrillation of TLCP phase was enhanced when the content of organoclay was 5 and 7%, relatively low compared to 30% of the solid-filler content in Refs. [35,36].

2. Experimental

2.1. Materials

The matrix polymer used in this work was nylon-6 (N6) with the trademark of Akulon F-x 9025, kindly supplied by DSM, The Netherlands. The thermotropic liquid crystalline polymer used was Vectra A950 (VA), wholly aromatic co-polyester of 73 mol% hydroxybenzoic acid (HBA) and 27 mol% hydroxynaphthoic acid (HNA) manufactured by Hoechst Celanese. Organophilic montmorillonite (OMMT) used in this study was prepared by using standard ion-exchange procedure and suitable for use with polyamides. The interlayer distance of the OMMT was about 1.92 nm measured by X-ray diffraction (XRD). Its organic content was about 32 wt% by measuring the weights loss up to 700 °C at a heating speed of 10 °C/min in nitrogen atmosphere.

2.2. Sample preparation

Prior to melt processing, N6 and VA pellets were dried at 110 °C under vacuum for at least 12 h. OMMT was first mixed with N6 at the weight ratio of 1/80, 3/80, 5/80 and 7/80 by using Haake RC90 equipped with a TW100 conical counter-rotating twin-screw extruder. The temperatures of barrel sections from the hopper to the die were set at 200, 210, 230 and 220 °C. The screw speed was fixed at 30 rev/min. According to the planned weight ratio, the weight percentages of OMMT in these binary composites were 1.23, 3.61, 5.88 and 8.04 wt%, respectively. The actual percentages of OMMT, determined by following the method introduced by Fornes et al. [23], were 1.12, 3.31,

5.19 and 7.25 wt% accordingly. The real OMMT percentages were slightly lower than the planned ones.

After pelletizing and drying, the obtained extrudates were further melting blended with VA by using the same extruder but with a different set of extrusion conditions. The temperature profile along the barrel of the extruder was: 240, 260, 285 and 280 °C. The measurement of melt temperatures showed that the real temperature at the end of extruder was 10 °C higher than the setting as a result of shear heating. So the temperature for the measurement of steady shear viscosities of N6, VA and N6/OMMT composites was selected as 290 °C. The screw speed was fixed at 40 rev/min, which corresponds to a shear rate of ca. 50 s^{-1} in the mixing section [37]. In this extrusion step, a straight die-head with 1 mm diameter and a length to diameter ratio (L/D) of 14 was used, and the maximum shear rate near the wall of the die-head was about 1×10^3 s^{-1}, calculated by using Poiseuille equation with the measured volume output of pure N6. The extruded strands were immediately quenched in a water bath (distance between the die-head and water bath $\approx$25 cm), and no post-drawing was applied after the extrusion. The extruded strands were pelletized and dried for further processing and characterization. For hybrid blends with clay content of 3 and 7 wt%, sampling was also performed at two positions inside the extruder by 'stopping machine' method. Position 1 was just at the end of the screws, and position 2 at the converging zone before the parallel section of the die.

2.3. Wide-angle X-ray diffraction (WAXD)

WAXD test was conducted by using a Rigaku D/max2500 diffractometer with Cu K_α radiation (λ= 0.15406 nm) with a 0.02 2θ step size and a 0.3 s count time. X-ray analysis was performed on a solid plate sample ($10\times10\times1$ mm^3 thick) prepared by melt pressing, except for the OMMT in powder form.

2.4. Rheological characterizations

Dynamic rheological measurements were performed by using a Rheometrics SR 200 dynamic stress rheometer. After compounding, the extrudates were injection-molded at 240 °C into 1 mm thick disks in a CS 183 Mini-Max Molder. The measurements were then run with a 25 mm parallel plate geometry and a 1 mm sample gap at 240 °C. Samples were placed between the preheated parallel plates and were allowed to equilibrate for 15 min before each measurement. The dynamic viscoelastic properties were determined within a range of frequencies from 0.1 to 500 rad/s, using strain values determined with a stress sweep to lie within the linear viscoelastic region. Experiments were carried out in nitrogen atmosphere to prevent oxidative degradation of the specimens.

Steady shear viscosities of N6, VA and N6/OMMT composites were measured at 290 °C using a Rosand RH7 capillary rheometer. The rheometer was equipped with a capillary having a diameter of 1 mm and a length of 30 mm. Entrance effects were neglected due to the high *L/D* ratio. The Rabinowitsch correction was applied to all measured results.

2.5. Morphology observation

The dispersion state of clay platelets was investigated by a TEM (Hitachi H-800, Japan) with an acceleration voltage of 100 kV. The ultrathin slices, approximately 70–90 nm thick, were obtained from samples for rheological tests by ultra-microtoming under cryogenic condition.

The extrudates of the blends containing VA were cryogenically fractured in liquid nitrogen and coated with gold before SEM investigation. The fracture surfaces of blends were observed with a SEM (Hitachi S-4300, Japan) at an accelerating voltage of 15 kV. Formic acid was used to dissolve the matrix selectively from the extrudates to clearly show the VA morphology and to measure the diameter of VA particles and fibrils in the blends. The selective dissolving process was the same as in a previous paper [35]. The diameters of VA particles were measured from SEM photos of the residues after selective dissolving by using the image analysis software (Image-Pro Plus 4.5, Media Cybernetics, Inc.). The average diameter for one sample was obtained from at least 300 particles.

2.6. Dynamic mechanical analysis

Dynamic mechanical analysis (DMA) was carried out by means of a Perkin–Elmer DMA-7 system. The plaques ($15\times5\times2$ mm^3) used for DMA test were injection-molded at 240 °C in a CS 183 Mini-Max Molder. All measurements were conducted in the three-point bending mode at a fixed frequency of 1 Hz and a heating rate of 5 °C/min from 10 to 200 °C.

3. Results and discussions

3.1. Dispersion of clay platelets in the composites

The dispersion state and nanostructure of clay platelets in a polymer layered silicate nanocomposite (PLSN) have dramatic influences on its mechanical, thermal and rheological performances. In this study, a good dispersion of clay platelets is basic for studying the interactions between the clay and the deformable TLCP phase.

Wide-angle X-ray diffraction (WAXD) and transmission electron microscopy (TEM) are the most commonly used techniques to elucidate the nanostructure of PLSNs [38]. Rheological measurement, as a complementary method, also offers a means to assess the dispersion state of clay platelets in the polymer matrix [39]. In this study, all the

three methods were used to show the microstructure of clay platelets in the composites.

Fig. 1 shows the XRD patterns of OMMT, the binary and ternary composites with different clay loadings. The diffraction patterns of the composites with the lowest clay loading are not shown in this figure, due to the low sensitivity of WAXD method at clay content ≤ 1 wt%. For the binary N6/OMMT composites with clay loadings of 3/80 and 5/80, the peak at $2\theta = 4.54°$ (d-spacing 1.92 nm) which ascribed to the reflection of d_{001} spacing of OMMT disappeared, indicating an exfoliated structure. When the clay loading was 7/80, the peak at 4.54° became broad and shallow. A new reflection peak appeared at $2\theta = 2.30°$ (d-spacing 3.84 nm). All the results indicate that a high degree of dispersion of clay platelets was reached by melt extrusion. For the ternary composites, no discernable peaks were observed in the WAXD patterns shown in Fig. 1. So it is believed that there was no re-aggregation of clay platelets after blending binary composites with VA. Even more, for the composite with OMMT content of 7 wt%, a further dispersion of clay occurred.

TEM photographs shown in Fig. 2 give a direct representation of microstructure for the selected composite (N6/OMMT 80/3) before and after blending with VA. TEM image at low-magnification (Fig. 2(a)) shows well dispersed clay throughout the matrix. The image at high-magnification (Fig. 2(b)) shows that the clay platelets are in exfoliated state, which is consistent with the WAXD results. The photograph after blending with VA (Fig. 2(c)) reveals that the second extrusion process enhanced the dispersion of clay platelets, indicated by further decreased thickness of the clay layers. It is believed that the enhanced dispersion is owing to the fact that the polymer molecules have more possibility to diffuse into the galleries of clay layers for their low viscosity at the high temperature of the second extrusion process.

Furthermore, dynamic rheological measurements were also carried out to examine the dispersion state of clay in the N6 matrix. The results are shown in Fig. 3. Fig. 3(a) shows logarithmic plots of storage moduli G' versus angular frequency ω at 240 °C for pure N6 and N6 nanocomposites

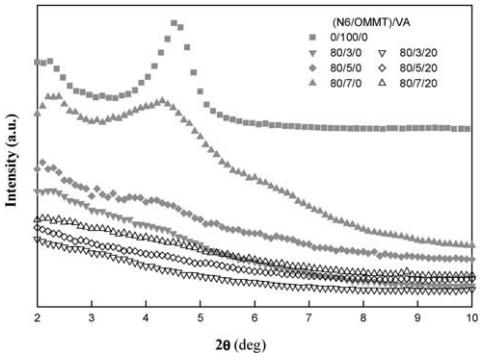

Fig. 1. WAXD plots for OMMT, N6 binary composites with different contents of OMMT and the corresponding ternary blends with 20 wt% VA.

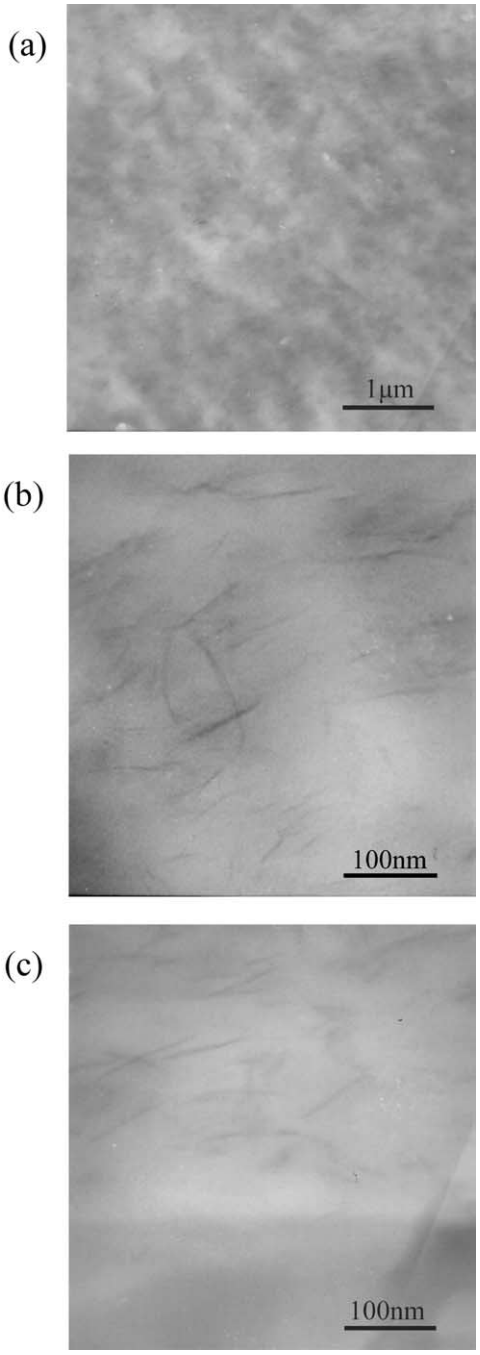

Fig. 2. TEM micrographs of N6 composite: (a) binary composite (N6/OMMT 80/3) at low-magnification and (b) high-magnification, (c) ternary hybrid blend (N6/OMMT/VA 80/3/20) at high-magnification.

with different clay loadings. As shown, the storage moduli of the nanocomposites show a monotonic increase at all frequencies with increasing silicate content. The G' of N6 matrix shows a near-terminal behavior ($G' \sim \omega^2$), while those of composites show a distinct non-terminal behavior similar to that observed for end-tethered nanocomposites [40]. That is to say, the frequency dependence of G' was weakened monotonically with the clay content at low frequencies. The solid-like behavior of the PLSN indicated

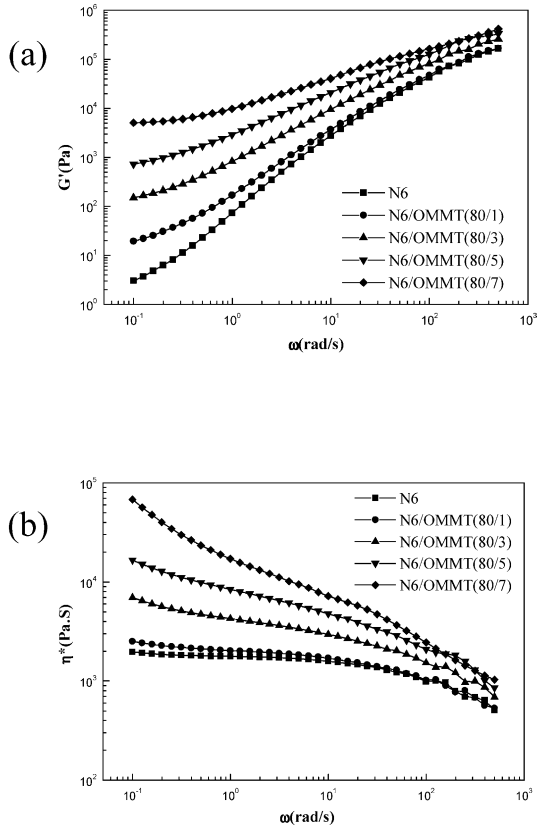

Fig. 3. (a) Storage modulus G' and (b) complex viscosity η^* versus frequency for N6 and N6/OMMT nanocomposites at various clay loadings (T=240 °C).

by the low-frequency response has been attributed to the formation of a percolated network superstructure in the nanocomposites [41,42]. Fig. 3(b) shows logarithmic plots of complex viscosity η^* versus angular frequency at 240 °C for pure N6 and N6 nanocomposites. It can be found that the complex viscosities of the composites increase with increasing clay loading, too. The composites with clay loading higher than 3/80 exhibit solid-like non-Newtonian flow behavior and show enhanced shear thinning feature. Though rheological method cannot distinguish the difference between intercalated and exfoliated structure [39], the significant changes in viscoelastic behavior indicate that the good dispersion state of silicate platelets in N6 matrix, too.

The results of WAXD, TEM investigations and rheological measurements presented above are consistent with each other. It is shown that the clay platelets were well dispersed by using the melt-extrusion method. So it is meaningful to study the influences of clay platelets on the morphology of the dispersed VA phase.

3.2. Influences of clay addition on the micro-rheology parameters

The polymer blending is a process that makes the minor phase dispersed uniformly into the matrix in the desired domain shape and size. The establishment of the morphology of polymer blends in blending equipments is a dynamic process. The complex processes, such as deformation, breakup, coalescence and relaxation are all involved in this process [37,43]. Two basic micro-rheology parameters are crucial to the deformation and breakup of the dispersed phase without the exception of the TLCP-containing blends. They are the viscosity ratio of the dispersed phase to the matrix, η_d/η_m, and the capillary number, Ca.

During the processing of binary TLCP/thermoplastics blends, the viscosity ratio of TLCP phase to the matrix is one of the most important factors governing the deformation and fibrillation of the TLCP phase. Many papers have reported on this topic. The majority of the published results indicate that the fibrillation is enhanced when the viscosity ratio of TLCP phase to the matrix is less than unity. It was also suggested that the viscosity ratio far below unity was needed for significant TLCP fibrillation at a lower TLCP content [44]. Thermoplastic matrices of low viscosities, such as polyamides and polyesters, have often been chosen as examples to demonstrate that TLCP is difficult to form fibrils in their blend melts with high viscosity ratios.

In the present study, during the blending of the TLCP with N6 or N6 composites, the TLCP content and the extrusion conditions were kept the same, so the morphological difference of TLCP phase should be related to the viscosity difference of the matrix and the addition of clay of different concentrations. Unambiguously, the viscosity difference of N6 matrices also had a direct relation with the addition of clay.

In order to investigate the possible influence of viscosity ratio on the TLCP fibrillation, we measured the apparent shear viscosities of N6, VA and N6/OMMT composites by using a capillary rheometer. In the calculation of the viscosity ratio of ternary hybrid N6/OMMT/VA blends, the following points were considered. In the filler-containing polymer blends, if the fillers had a good compatibility with one of the polymers, they could be taken as one phase. In a nano-silica filled PP/TLCP system, Hu et al. took the PP and hydrophobic nano-silica as the matrix phase in the discussion on the viscosity ratio of the matrix to the dispersed TLCP phase [19]. During the studying of the influences of glass spheres on the phase inversion concentration of PS/PMMA blends, the component consisting of PMMA and glass spheres in the blends was treated as one ‘PMMA-phase’ because of the selective filling of filler in the PMMA [45]. In these studies, reasonable conclusions were reached by using such assumption. In the present study, nylon matrix and silicate platelets were prefabricated before blending with VA and in good miscibility due to the presence of strong hydrogen bonds between them. So the migration of silicate platelets from nylon to VA phase was difficult only in the several minutes starting from adding solid polymer pellets to extruding the melt out of the die. This was confirmed by energy dispersion X-ray analysis

on the fracture surface of the extrudates by using a SEM. It indicated that little silicate platelets were located in VA phase, while most of them in the nylon matrix. So in the later discussion, the melt of N6/OMMT composite was treated as a whole equivalent medium.

The viscosity values of N6 and N6 with different clay loadings at the shear rates of 50 and 1000 s^{-1}, the two typical shear rates encountered during the extruding process, are shown in Fig. 4. The straight lines are the weighted linear fitting results of the viscosity as a function of the clay concentration. The viscosities of pure VA at these two shear rates are also indicated as the dotted lines in the same figure.

Compared to the oscillatory test, relatively few investigations devoted the attention to the steady shear properties of polymer nanocomposite [39]. The investigation of Fornes et al. on nylon-6 nanocomposites revealed that the viscosities of nanocomposites were lower than the pure matrix in the shear rate range of 10–200 s^{-1} [23]. Our results agreed well with them on this point. The result shown in Fig. 4 indicates that the viscosities of nanocomposites are lower than the pure matrix at the shear rate of 50 and 1000 s^{-1}. The viscosities of composites at these two shear rates have decreasing tendency with increasing clay concentration, as shown by the linear fitting curves. The decrease is more significant at shear rate 1000 s^{-1}. The viscosity ratios of VA to the matrix at these two shear rates are in the range of 0.36–1.27. Based on this, it can be said that the fibrillation of VA is still possible, although the addition of clay has the tendency to decrease the viscosity of the matrix.

Besides the viscosity ratio, the deformation and breakup of the dispersed VA droplets also depend on another dimensionless parameter, the capillary number, Ca. It is the ratio of the viscous stress that tends to deform the droplet to the interfacial tension that tends to keep the droplet spherical. In the simple shear flow, it is defined as

$$\mathrm{Ca} = \frac{\text{Hydrodynamic stress}}{\text{interfacial stress}} = \frac{\eta_m \dot{\gamma}}{\sigma/R} \quad (1)$$

where η_m is the matrix viscosity, $\dot{\gamma}$ the shear rate, R the droplet radius, and σ the interfacial tension of polymer pairs.

For capillary numbers above a critical value (critical capillary number, Ca_{crit}), the droplet can no longer sustain continuous deformation, and it breaks up eventually. The values of Ca_{crit} strongly depend on the viscosity ratio and the type of flow (shear or elongation). Ca_{crit} as a function of viscosity ratio (p) in shearing flow can be calculated from an empirical equation [46]:

$$\log(Ca_{crit}) = -0.5060 - 0.0994 \log p + 0.1240(\log p)^2 - 0.1150/(\log p - 0.6110) \quad (2)$$

When the viscosity ratios were in the range of 0.36–1.27, Ca_{crit} for each blend was almost in the same value as 0.48 ± 0.02. It indicated that the viscosity change of the matrix had almost no influence on the value of Ca_{crit} in this study.

Depending on the ratio of Ca to Ca_{crit}, the dispersed droplets will either deform or breakup according to the criteria summarized by Utracki et al. [46] in both shear and elongation flow field. The criteria have been used by Isayev et al. to predict the morphology development during fiber spinning of polyesters and TLCP blends [47]. The detailed recitation of the criteria is not present here. But it is deserved to note that when $Ca/Ca_{crit} > 4$, the droplets will deform affinely into long stable filaments. It is the criterion that should be satisfied if the TLCP phase is wanted to form fibrils with large aspect ratio in a TLCP/thermoplastic blend.

Given the decreasing matrix viscosity and unchanged Ca_{crit} with the increase of clay concentration, the addition of clay into N6/VA seems unfavorable to the fibril formation of TLCP phase in the hybrid blends. What is the scenario in actual melt blending process?

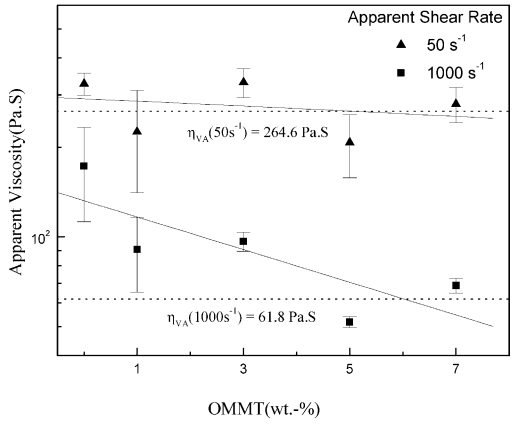

Fig. 4. Steady shear viscosity of N6 and N6/OMMT composites with different clay concentrations at shear rate of 50 s^{-1} (▲) and 1000 s^{-1}(■) measured by using a capillary rheometer (T=290 °C). The straight lines are the weighted linear fitting results of the viscosity as the function of the clay concentration. The viscosities of VA at the two shear rates are indicated as the dotted lines.

3.3. Morphology evolution of dispersed TLCP phase with the increase of clay content

Here, most of the attention is given to the final morphology of the extrudates. Because the final morphology of the polymer blends depends on the factors such as the processing parameters, properties of component polymers and compositions of the blends. The processing parameters were kept the same in this study, so the morphological difference could be correlated well with the variation of the composition of hybrid blends.

3.3.1. TLCP morphology in extruded polyblends

SEM micrographs of the fracture surface of (N6/OMMT)/VA extrudates are shown in Figs. 5–7. These

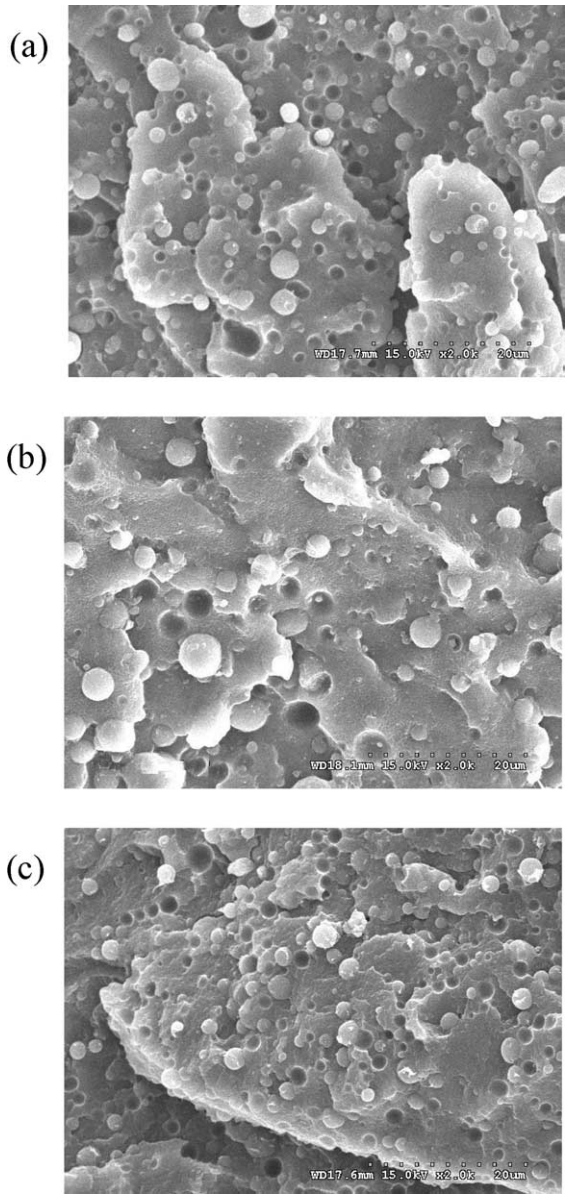

Fig. 5. SEM micrographs of fracture surfaces for the blends of N6 nanocomposites and VA, the weight percent of VA in the blends is always 20 wt% and OMMT loading is: (a) 0 wt%, (b) 1 wt%, (c) 3 wt% (relative to the weight of polymeric based materials).

pictures show the morphology of binary and ternary blends with different OMMT loadings, with the blending ratio of N6/VA kept at 80/20. It should be emphasized that no post-drawing was applied on the extrudates after melt extrusion.

When the OMMT content in the ternary blends was $\leq$3 wt%, the VA in the fracture surface was mainly in the form of spheres (Fig. 5(a)–(c)). In order to investigate the effect of clay loading on the size of dispersed VA droplets, a comparison of the size distributions was conducted based on the SEM image analysis of the residues after the selective dissolving of N6 with formic acid. The number-average diameter (D_n) and volume-average diameter (D_V) were calculated by using the following relations:

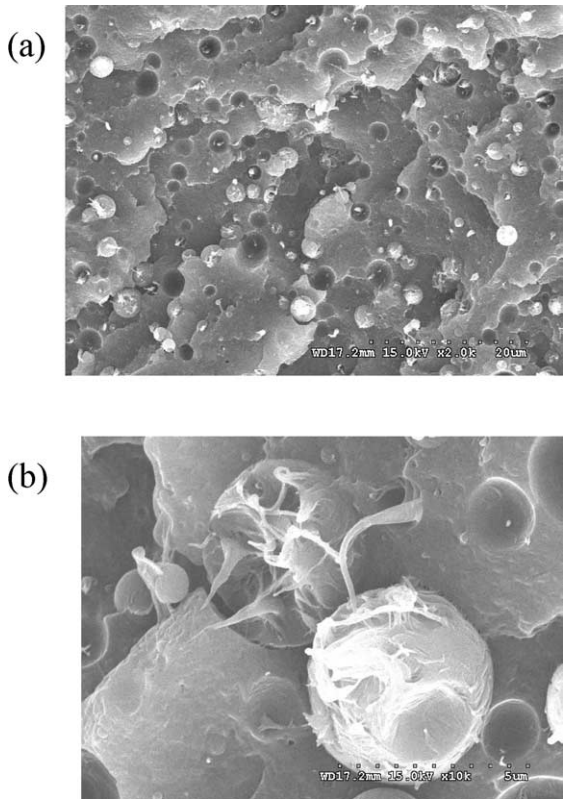

Fig. 6. SEM micrographs of fracture surface for (N6/OMMT)/VA (80/5)/20 ternary blend at the magnification of (a) ×2000 and (b) ×10,000.

$$D_n = \frac{\sum_i n_i d_i}{\sum_i n_i} \tag{3}$$

$$D_V = \frac{\sum_i n_i d_i^4}{\sum_i n_i d_i^3} \tag{4}$$

with n_i as the number of spheres having diameter d_i.

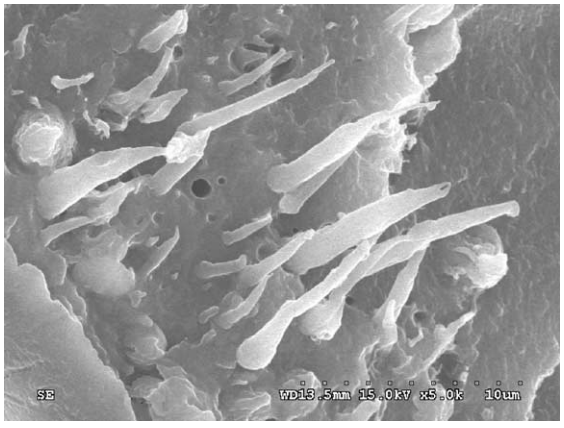

Fig. 7. SEM photograph of fracture surface of the (N6/OMMT)/VA (80/7)/20 ternary blend.

Table 1
Statistic results of VA particle size distribution for blends with clay loading <3 wt%

(N6/OMMT)/VA	D_n	D_V	D_V/D_n
(80/0)/20	2.04	2.75	1.35
(80/1)/20	1.68	2.6	1.55
(80/3)/20	1.14	1.95	1.71

Dispersed VA phase is mainly in the form of droplets in these blends.

Concluded from the statistic results (Table 1), D_n and D_V decreased with increasing clay content, while the polydispersity of the droplet size increased somewhat with increasing clay content.

When the organoclay content increased to 5 wt%, VA spheres and fibrils co-existed on the fracture surface (Fig. 6(a)). Though this photograph was in the same magnification as those in Fig. 5, the details of the VA morphology were not distinguishable. A close look at high magnification (×10,000) more clearly revealed that fine VA microfibrils dispersed in N6 matrix and some microfibrils having diameters of 300–500 nm formed from the dispersed VA spheres (Fig. 6(b)). A similar morphology was found in an N6/TLCP/EPDM-*g*-MAH blend [48]. But the present result was generated with the addition of nano-clay, instead of the maleated EPDM compatibilizer.

When clay content increased to 7 wt%, more VA fibrils were formed (Fig. 7). Their average diameters were about 1 μm. Usually, the formation of TLCP fibrils with large aspect ratios in a N6 matrix is a difficult job. In N6/Vectra B950 system, as reported by La Mantia et al., TLCP phase formed very little fibril structure at the fracture surface of extrudate even at a high draw ratio of 100, although the elongation field was believed to be efficient to deform the dispersed TLCP phase into fibril structure [49]. Here, VA phase was deformed into fibrils of large aspect ratio without any post-drawing. It was caused mainly by the shear action in the channel of the die and with the presence of nano-clay.

3.3.2. TLCP morphology difference before and after die

In order to depict the morphology evolution with the clay concentration in more detail, the sampling of N6/OMMT/VA blends of different clay-loadings was conducted at different positions of the extruder, as shown in Fig. 8.

For the hybrid blends with clay concentration of 3 wt%, no deformation of the VA droplets was found at the positions before and after the die. The dispersed phase was in the form of spheres but in different sizes. At position 1, where just after the mixing zone of the extruder, the VA particles had an average diameter D_n of 2.65 ± 0.87 μm. After flowing through the die, the sample still had no fibrils as shown in Fig. 5(c). The average diameter of the TLCP spheres became 1.14 ± 0.54 μm. The decrease of the particle size was caused by the high shear rate that the melt experienced in the die.

In contrast, a different morphology development occurred for the hybrid sample with clay content of 7 wt%. As shown in Fig. 8(b), most of the VA particles were in the form of sphere at position 1. Their size distribution was somewhat large, as a result of unsteady transition during the breakup and relaxation process. The sample at position 2 in the converging zone had more deformed VA particles (Fig. 8(c)). After flowing through the die, very long VA fibrils were formed (Fig. 8(d)).

For the hybrid blends with different clay concentrations, the morphological investigation revealed that the morphological differences existed not only in the final extrudates after the die, but also in the samples obtained before the die. Inside the extruder, the VA phase had a deformed morphology in hybrid blend with 7 wt% clay filling, while not in the blend with 3 wt% clay. For the blend with 7 wt% clay, the sampling at different positions showed that the extensional flow at the converging zone played a role to deform the VA particles, but the VA fibrils were mainly generated inside the channel of the die and further developed due to the action of shear field.

3.4. Mechanism of the enhanced TLCP fibrillation

In this study, the nylon-6 was viscous and the viscosity ratio of VA to nylon-6 was less than unity at the shear rates encountered in the extrusion process. The viscosity ratio should favor the fibril formation of VA in this nylon matrix. Using the criteria suggested by Utracki et al. to estimate the deformation and breakup behaviors of VA droplets, the capillary number for N6/VA binary blends at shear rates of 50 and 1000 s^{-1} was calculated. For the calculation, the shear stress (τ) at the corresponding shear rate was obtained from $\tau = \eta\dot{\gamma}$. The resulting shear stresses exerted by N6 during processing were approximately 16.4 kPa at 50 s^{-1} and 173 kPa at 1000 s^{-1}. The radius of dispersed particles of 0.5 μm was used, which was the low limit of the average particle size in both binary and ternary blends. The dispersed particles with size larger than this had more possibility to be deformed at the action of same shear stress, because Ca is directly proportional to the radius of dispersed particles, R. The interfacial tension between N6 and VA is hard to obtain because of the experimental difficulty in measuring the interfacial tension between these two polymer melts. Most of TLCPs have quite high melting temperatures, so that the thermal degradation of the other component polymers is severe and unavoidable at high temperatures for measuring the interfacial tension between polymer pairs containing a TLCP (e.g. VA used here). Furthermore, there are still some doubts about the applicability of existing techniques for measuring the interfacial tension between TLCP and other polymers, caused by the unique viscoelasticity and the molecular chain orientation of the TLCP phase [50], although their interfacial tension values obtained by using these methods are still available in the published reports [51,52]. Recently,

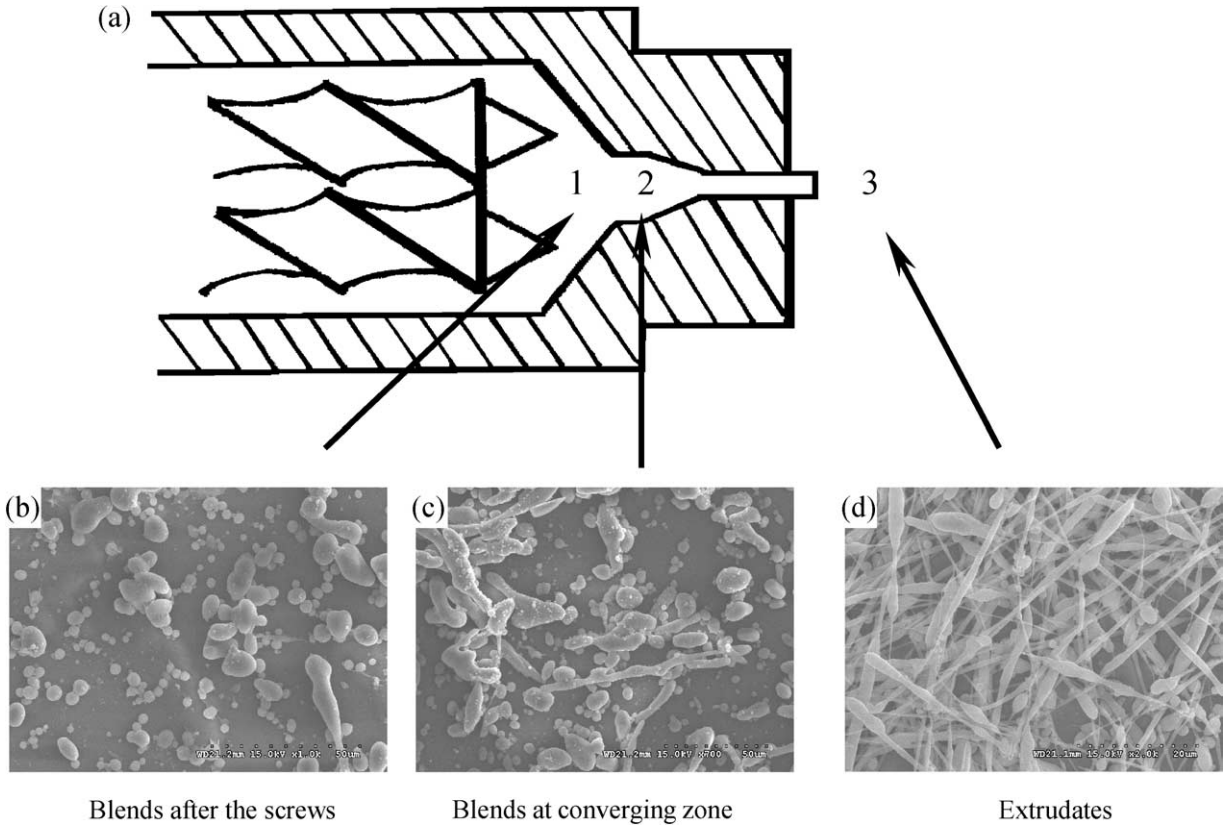

Fig. 8. Morphology development of VA phase in (N6/OMMT)/VA (80/7)/20 ternary blend after the mixing zone in the extruder; (a) is the schematic representation of the positions from which samples were obtained for morphology investigation; (b), (c) and (d) are SEM photographs of the VA phase after extraction of nylon-6 matrix. They are corresponding to the sampling positions 1, 2 and 3, respectively.

Zhou et al. observed a dynamic interfacial process between PC and a TLCP (LC-5000, a co-polyester of PET-PHB80) by measuring the time-dependent interfacial tension between them. They attributed this status to the relaxation of stretched domains inside the TLCP drops [53]. This also brought on the complexity in measuring the interfacial tension between common thermoplastics and TLCP. We also referred to the experimentally measured values between the immiscible polymer pairs, such as PS/PA6 (6.8–8.4 mN/m) [50], PES/Vectra A900 (4–6 mN/m) [51], PP/Vectra A950 (23.5 mN/m) [52]. Finally, for a reasonable and acceptable resolution, the interfacial tension between N6 and VA was taken as 10 mN/m in our calculation. The capillary numbers for the binary N6/VA (80/20) blend could be calculated from Eq. (1) with above values. The capillary numbers at 50 and 1000 s^{-1} were 0.82 and 8.6, respectively.

As stated in Section 3.2, the critical capillary numbers at these two shear rates were the same of 0.48. So the ratios of Ca to Ca_{crit} at these shear rates were 1.7 and 18.0, respectively. According to the criteria suggested by Utracki et al., the deformation of VA phase should have occurred in the extrusion of N6/VA blend, because the condition of $Ca/Ca_{crit} \gg 4$ was satisfied when the polymer blends flowed through the die. But there was no sign of fibrils formed during the extrusion of the binary blend. This indicated that the shear stress was not effectively transferred from the matrix to the dispersed phase.

Vectra A950 and nylon-6 is a pair of immiscible polymers. In their blends, the interfacial slip exists between the dispersed phase and the matrix. This interfacial slip originates from the lower chain entanglements at the interface of two immiscible polymers, and it is evident especially for TLCP-containing blends due to the molecular rigidity and orientation ability of TLCPs [54]. In a multiphase system, the local shearing stress at the droplet surface may be assumed to be continuous, even in the systems appearing strong interfacial slip [54,55]. However, the discrepancy between the experimental results and the prediction based on the calculated values showed that the shear stress imposed on the matrix was not effectively transferred to the dispersed VA phase in the N6/VA binary blends, especially at the high shear rate encountered during the extrusion process.

For the blends containing organoclay, the viscosity ratios of VA to the matrixes were still in the vicinity of unity, though the addition of clay reduced the viscosity of the matrixes. The same calculation procedure was performed to investigate the relative magnitude of Ca and Ca_{crit} for clay-containing hybrid blends. It was found that the ratios of Ca to Ca_{crit} in the hybrid blends were the same as the case in the

binary N6/VA blend. Inside the extruder, $1 < Ca/Ca_{crit} < 4$, which meant the dispersed droplets will deform and break conditionally [46,47]. When the melts flowed through the die, in the case of $Ca/Ca_{crit} \gg 4$, the dispersed droplets would have deformed affinely into long stable filaments [46,47]. However, from the morphological investigation, it was concluded that the real morphology in the hybrid blends with clay concentration less than 3 wt% still could not be correlated well with the prediction based on the calculated results of Ca/Ca_{crit}. But the final size of dispersed particle decreased with increasing clay concentration. It indicated that the shear action experienced by the dispersed VA phase increased with the increase of clay concentration. With the clay concentration up to 5 and 7 wt%, the experimental results and theoretical predication were in accordance with each other very well. As shown in Fig. 8, the VA droplets in (N6/OMMT)/VA (80/7)/20 hybrid blend were deformed inside the extruder and further to fibrils with large aspect ratios out of the die.

The morphological evolution of dispersed VA particles indicated the efficiency of shear stress transferring gradually increased with increasing clay concentration in the blends. The efficient stress transfer occurred as a result of the increased adhesion and suppressed interfacial slip between VA and nylon matrix by the well-dispersed clay platelets. The better adhesion between TLCP and the matrix also prevented the dispersed VA phase from tumbling, thus more energy was used for the breakup and deformation [56]. So the clay also played the role as a compatibilizer in this study.

However, the enhanced fibril formation did not imply the increased thermodynamic compatibility between N6 and VA phase, as reported on the similar systems with the addition of reactive compatibilizers instead of clay platelets [48,57], and some organoclay filled immiscible blends without a TLCP [25]. Here, DMA tests were performed for N6, N6/VA blend and N6/OMMT/VA ternary blends. The glass transition temperature (T_g) of N6 in each system was detected from the plots of damping factor (tan δ) versus temperature. T_g values of VA could not be detected because no discernable peak appeared around 100 °C where the glass transition of VA was believed to take place. T_g values and the height of corresponding tan δ peaks that belong to N6 are shown in Table 2. It can be clearly seen that the addition of organoclay has little influence on T_g of N6 in the blends. This indicates that the addition of organoclay did not improve the thermodynamic compatibility between VA and N6. However, the addition of VA component decreased the height of damping peaks. These heights also decreased with the increase of clay content in the hybrid blends. The height of damping peak represents the motion ability of polymer chains. Its decrease indicated the clay and VA inclusions restricted the movement of polymer molecules. The restriction came from two origins: the increase of clay content and the formation of TLCP fibrils at high clay contents. These two factors also had influences on the mechanical properties of the resulted materials. Fig. 9 shows the storage modulus as a function of temperature for N6 and N6/VA blends with different clay contents. The modulus of the blends increased with the addition of VA and clay platelets. The increase was especially evident when the modulus in the rubbery region was taken into consideration.

Table 2
Glass transition temperatures (T_g) of nylon-6 measured by DMA test, and the heights of corresponding peaks in the damping curves

(N6/OMMT)/VA	T_g (°C)	Peak height
100/0/0	68	0.145
80/0/20	70	0.127
80/1/20	70	0.122
80/3/20	69	0.110
80/5/20	69	0.107
80/7/20	68	0.099

4. Concluding remarks

The morphology of minor TLCP phase was influenced by well-dispersed nano-clay in nylon-6 matrix. As an immiscible pair, the blend of VA and N6 had interfacial slip between the dispersed VA droplets and the N6 matrix. The inefficient shear transfer hindered the formation of VA fibrils in the binary N6/VA blend. While in the ternary N6/OMMT/VA blends, the size of VA droplets decreased with increasing clay content when the clay content was $\leq$3 wt%, and VA droplets were deformed into fibrils with large aspect ratio when the clay content increased to 7 wt%. Morphological investigation of the samples obtained inside the extruder also revealed that the fibrillation of VA phase occurred inside the extruder for the hybrid blend of 7 wt% clay.

Due to the presence of nano-clay particles, especially at 7 wt% loading, the morphology evolution of VA was consistent well with the prediction by the criteria based on the ratio of Ca to Ca_{crit}. The morphological change of the VA phase with the addition of clay was attributed to the improved interfacial adhesion by the clay platelets and

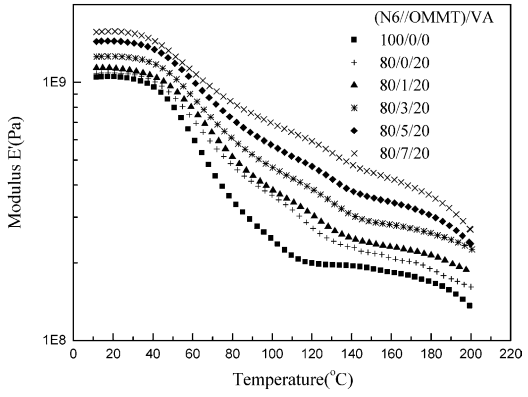

Fig. 9. The variation of storage modulus versus temperature for N6 and N6/VA blends at various clay loadings.

the suppressed interfacial slip between VA and nylon. So the shear stress could be effectively transferred from nylon to the dispersed VA phase to enhance its deformation and fibrillation.

Acknowledgements

The work is financially supported by the National Natural Science Foundation of China (Grant No. 50233010) and the Outstanding Overseas Chinese Scholars Fund of Chinese Academy of Sciences. The authors would like to express their appreciation to DSM Research, The Netherlands, for their supplying of nylon 6.

References

[1] Jackson Jr WJ, Kuhfuss HF. J Polym Sci, Polym Chem Ed 1976;14(8):2043–58.
[2] Dutta D, Fruitwala H, Kohli A, Weiss RA. Polym Eng Sci 1990;30(17):1005–18.
[3] Roetting O, Hinrichsen G. Adv Polym Tech 1994;13(1):57–64.
[4] Handlos AA, Baird DG. J Macromol Sci, Rev C 1995;35(2):183–238.
[5] Tjong SC. Mater Sci Eng, R 2003;41(1–2):1–60.
[6] Baird DG, Wilkes GL. Polym Eng Sci 1983;23(11):632–6.
[7] Cogswell FN, Griffin BP, Rose JB. US Patent No. 4433083; 1984.
[8] Bafna SS, De Souza JP, Sun T, Baird DG. Polym Eng Sci 1993;33(13):808–18.
[9] He JS, Zhang HZ, Li G, Xu XQ. Acta Polym Sin 1993;(1):115–9.
[10] Kulichikhin VG, Parsamyan IL, Lipatov YS, Shumsky VF, Getmanchuk IP, Babich VF, et al. Polym Eng Sci 1997;37(8):1314–21.
[11] He JS, Zhang HZ, Wang YL. Polymer 1997;38(16):4279–83.
[12] He JS, Wang YL, Zhang HZ. Compos Sci Technol 2000;60(10):1919–30.
[13] Pisharath S, Wong SC. Polym Compos 2003;24(1):109–18.
[14] Garcia M, Eguiazabal JI, Nazabal J. Compos Sci Technol 2003;63(15):2163–70.
[15] Shumsky VF, Lipatov YS, Kulichikhin VG, Getmanchuk IP. Rheol Acta 1993;32(4):352–60.
[16] Tchoudakov R, Narkis M, Siegmann A. Polym Eng Sci 2004;44(3):528–40.
[17] Tjong SC, Meng YZ. Polymer 1999;40(26):7275–83.
[18] Shumsky VF, Getmanchuk IP, Lipatov YS. J Appl Polym Sci 2000;76(7):993–9.
[19] Lee MW, Hu X, Yue CY, Li L, Tam KC, Nakayama K. J Appl Polym Sci 2002;86(8):2070–8.
[20] Lee MW, Hu X, Yue CY, Li L, Tam KC. Compos Sci Technol 2003;63(3–4):339–46.
[21] Fornes TD, Paul DR. Polymer 2003;44(17):4993–5013.
[22] Yoon PJ, Fornes TD, Paul DR. Polymer 2002;43(25):6727–41.
[23] (a) Fornes TD, Yoon PJ, Keskkula H, Paul DR. Polymer 2001;42(25):9929–40.
(b) Fornes TD, Yoon PJ, Keskkula H, Paul DR. Erratum. Polymer 2002;43(7):2121–2.
[24] Shah RK, Paul DR. Polymer 2004;45(9):2991–3000.
[25] Voulgaris D, Petridis D. Polymer 2002;43(8):2213–8.
[26] Schmidt D, Shah D, Giannelis EP. Curr Opin Solid State Mater Sci 2002;6(3):205–12.
[27] Mehrabzadeh M, Kamal MR. Can J Chem Eng 2002;80(6):1083–92.
[28] Gelfer MY, Song HH, Liu LZ, Hsiao BS, Chu B, Rafailovich M, et al. J Polym Sci, Part B: Polym Phys 2003;41(1):44–54.
[29] Wang Y, Zhang Q, Fu Q. Macromol Rapid Commun 2003;24(3):231–5.
[30] Khatua BB, Lee DJ, Kim HY, Kim JK. Macromolecules 2004;37(7):2454–9.
[31] Ray SS, Pouliot S, Bousmina M, Utracki LA. Polymer 2004;45(25):8403–13.
[32] Liu LM, Qi ZN, Zhu XG. J Appl Polym Sci 1999;71(7):1133–8.
[33] Cho JW, Paul DR. Polymer 2001;42(3):1083–94.
[34] Fornes TD, Yoon PJ, Hunter DL, Keskkula H, Paul DR. Polymer 2002;43(22):5915–33.
[35] Zheng XJ, Zhang J, He JS. J Polym Sci, Part B: Polym Phys 2004;42(9):1619–27.
[36] Ding YF, Zhang J, Chen P, Zhang BQ, Yi ZQ, He JS. Polymer 2004;45(23):8051–8.
[37] Sundararaj U, Macosko CW. Macromolecules 1995;28(8):2647–57.
[38] Morgan AB, Gilman JW. J Appl Polym Sci 2003;87(8):1329–38.
[39] Krishnamoorti R, Yurekli K. Curr Opin Colloid Interface Sci 2001;6(5–6):464–70.
[40] Krishnamoorti R, Giannelis EP. Macromolecules 1997;30(14):4097–102.
[41] Hoffmann B, Kressler J, Stöppelmann G, Friedrich C, Kim GM. Colloid Polym Sci 2000;278(7):629–36.
[42] Lim ST, Lee CH, Choi HJ, Jhon MS. J Polym Sci, Part B: Polym Phys 2003;41(17):2052–61.
[43] Utracki LA, Shi ZH. Polym Eng Sci 1992;32(24):1824–33.
[44] He JS, Bu WS, Zhang HZ. Polym Eng Sci 1995;35(21):1695–704.
[45] Steinmann S, Gronski W, Friedrich C. Polymer 2002;43(16):4467–77.
[46] Huneault MA, Shi ZH, Utracki LA. Polym Eng Sci 1995;35(1):115–27.
[47] Song CH, Isayev AI. Polymer 2001;42(6):2611–9.
[48] Seo Y. J Appl Polym Sci 1997;64(2):359–66.
[49] La Mantia FP, Saiu M, Valenza A, Paci M, Magagnini PL. Eur Polym J 1990;26(3):323–7.
[50] Xing PX, Bousmina M, Rodrigue D, Kamal MR. Macromolecules 2000;33(21):8020–34.
[51] Machiels AGC, Busser RJ, Van Dam J, Posthuma de Boer A. Polym Eng Sci 1998;38(9):1536–48.
[52] Gao P, Mackley MR, Zhao DF. J Non-Newtonian Fluid Mech 1999;80(2–3):199–216.
[53] Yu RB, Yu W, Zhou CX, Feng JJ. J Appl Polym Sci 2004;94(4):1404–10.
[54] Lam YC, Jiang L, Li L, Yue CY, Tam KC, Hu X. J Polym Sci, Part B: Polym Phys 2004;42(2):302–15.
[55] Jiang L, Lam YC, Yue CY, Tam KC, Li L, Hu X. J Appl Polym Sci 2003;89(6):1464–70.
[56] Seo Y. Macromol Symp 1999;147(1):201–8.
[57] Meng YZ, Tjong SC. Polymer 1998;39(1):99–107.